2011

Room-temperature ferromagnetism in graphitic petal arrays

Chandra Sekhar Rout
Purdue University, crout@purdue.edu

Anurag Kumar
Purdue University - Main Campus, kumar50@purdue.edu

Nitesh Kumar
Jawaharlal Nehru Centre for Advanced Scientific Research

A. Sundaresan
Jawaharlal Nehru Centre for Advanced Scientific Research

Timothy S. Fisher
Purdue University, tsfisher@purdue.edu

Rout, Chandra Sekhar; Kumar, Anurag; Kumar, Nitesh; Sundaresan, A.; and Fisher, Timothy S., "Room-temperature ferromagnetism in graphitic petal arrays" (2011). *Birck and NCN Publications.* Paper 764.
http://dx.doi.org/10.1039/c0nr00870b

Nanoscale

View Online
Dynamic Article Links

Cite this: *Nanoscale*, 2011, **3**, 900

www.rsc.org/nanoscale

COMMUNICATION

Room-temperature ferromagnetism in graphitic petal arrays

Chandra Sekhar Rout,[a] Anurag Kumar,[a] Nitesh Kumar,[b] A. Sundaresan[b] and Timothy S. Fisher*[a]

Received 15th November 2010, Accepted 25th December 2010
DOI: 10.1039/c0nr00870b

We report room-temperature ferromagnetism of graphitic petal arrays grown on Si substrates by microwave plasma chemical vapor deposition without catalyst. The samples have been characterized by Raman and X-ray photoelectron spectroscopy to confirm the absence of possible ferromagnetic impurities. The petals exhibit ferromagnetic hysteresis with saturation magnetization of ~4.67 emu cm^{-3} and coercivity of ~105 Oe at 300 K, comparable to the reported behavior of few-layer graphene. Upon O_2 annealing the saturation magnetization and coercivity decreased to 2.1 emu cm^{-3} and ~75 Oe respectively. The origin of ferromagnetism is believed to arise from the edge defects and vacancies in the petals.

Magnetism in carbon-based nanomaterials has attracted much interest recently both for basic physical understanding of the material and possible use in spintronic devices. These materials, including carbon nanotubes, fullerenes and single-layer graphene, can exhibit ferromagnetism at low-temperature and some above room temperature due to the electronic instabilities caused by bonding defects and the presence of unpaired electron spins in the graphitic network.[1–3] However, quantitative understanding of the origin of ferromagnetism in carbon nanomaterials, which contain only s and p electrons in contrast to traditional ferromagnets based on 3d or 4f electrons, still remains unresolved. A mixture of sp^2 and sp^3 coordinated atoms can exhibit ferromagnetic behavior due to the induced sp^3/sp^2 defect, the existence of zig-zag edges or the presence of a curved graphitic surface containing seven or eight membered rings.[3] The present work considers a graphite-based material with a high density of vertically oriented, exposed edges and provides related measurements of ferromagnetism as a contribution to the emerging body of experimental data related to this phenomenon.

Recent density functional theory (DFT) results predict that point defects in graphite such as vacancies and hydrogen-terminated edges are magnetic.[4,5] Several groups have reported room-temperature ferromagnetism in highly oriented pyrolytic graphite materials (HOPG).[6–9] By magnetic force microscopy, Pardo *et al.* established that the magnetic properties of the HOPG-based materials are related to topographic defects in the otherwise pristine material.[7] Esquinazi *et al.* reported that HOPG samples bombarded with protons appeared ferro- or ferri-magnetic with a stable magnetic ordering at room temperature.[9] Talapatra *et al.* reported that ion irradiation of nanodiamond with ^{15}N and ^{12}C can cause ferromagnetism caused by extensive defect generation in the lattice.[10] Cervenka *et al.* provided direct evidence of ferromagnetic order in HOPG with magnetic force microscopy and in bulk magnetization measurements at room temperature; the observed ferromagnetism was attributed to localized electron states at grain boundaries established by two-dimensional arrays of point defects.[11] Recent reports on the ferromagnetic properties of graphene and ferromagnetic ordering suggest that various defects, such as vacancies, topological defects or frustration, hydrogen chemisorption and adsorbed oxygen species, could be primary contributors.[12,13]

In this paper, thin graphitic petals were grown on Si (100) substrates through adaptation of a previously reported procedure used on carbon fibers and Ti-coated Si.[14,15] Uniform growth of petals was obtained under microwave plasma chemical vapor deposition (MPCVD) conditions of H_2 (50 sccm) and CH_4 (10 sccm) as the primary feed gases at 30 Torr total pressure and 700 W plasma power with 900 °C substrate temperature. A field emission scanning electron microscope (FESEM; Hitachi S4800) was used to characterize the morphology of the petals. Petal thicknesses were measured from the image profiles collected from a Veeco atomic force microscope (AFM). Raman spectra of the petals were collected by using a Bruker Senterra Raman confocal microscope with excitation source of 532 nm. XPS investigation occurred in an AXIS ULTRA DLD system under ultra vacuum (<10^{-9} Torr) conditions with a lateral resolution of 5 μm. Magnetic measurements were performed using a vibrating sample magnetometer (VSM) option in a Physical Properties Measurement System (PPMS, Quantum Design, USA).

Fig. 1 shows FESEM images of graphitic petals grown for 30 min on a Si (100) substrate. The typical height of the petals array grown from the Si surface was ~500 nm whereas the lateral edge length of

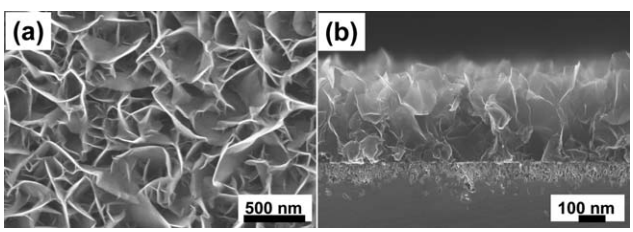

Fig. 1 FESEM image of graphitic petals grown on a Si substrate: (a) top and (b) cross-sectional views.

[a]*Birck Nanotechnology Center and School of Mechanical Engineering, Purdue University, West Lafayette, IN, 47907, USA. E-mail: tsfisher@purdue.edu*
[b]*Chemistry and Physics of Materials Unit, Jawaharlal Nehru Centre for Advanced Scientific Research, Jakkur P.O., Bangalore, 560064, India*

the petals varied between 200 and 1000 nm, and growth was uniform over the 1 × 1 cm^2 substrate. SEM analysis reveals that approximately ~4 × 10^8 interconnected petal edges are present in the 1 × 1 cm^2 sample area. Petal thicknesses in the range 1–10 nm from atomic force microscopy are consistent with previously reported morphologies corresponding to 5–25 graphene layers.[14,15] A Raman spectrum of the petal-decorated surface is shown in Fig. 2(a). The obtained Raman spectrum exhibits the characteristic peaks of few-layer graphene with no impurity peaks.[16,17] A G band near 1580 cm^{-1}, a D band near 1350 cm^{-1}, a 2D band near 2700 cm^{-1}, a weak 2D′ band near 3240 cm^{-1}, and D + G and 2D + G bands near 2950 and 4290 cm^{-1} are clearly apparent. The D band is a disorder-related defect Raman mode associated with transverse optical (TO) lattice vibrations near the *K*-point.[14] The mode observed near 2702 cm^{-1} is the result of second-order Raman scattering involving TO phonons near the *K*-point. Because the I_D/I_G and I_G/I_{2D} ratios are ~0.49 and 1.02 respectively and the intensity of the 2D mode is lower than the G-band intensity, the majority of petals here are expected to contain at least 5 layers.[17]

We have employed XPS to reveal surface elements and chemical bonding information, and to confirm that the sample is free from any other magnetic impurities. Only C and O peaks exist in the survey-scan XPS spectrum with no magnetic impurities as low as 0.01 at%, and the peak positions are consistent with prior literature.[18] Fig. 2(b) shows the obtained XPS spectrum, highlighting the C 1s and O 1s peaks from the graphitic petals. The C 1s peak can be precisely deconvoluted into three Gaussian peaks as shown in Fig. 2(b). The main peak centered at a 284.7 eV is assigned to sp^2 bonds, and the secondary peak at 285.2 eV corresponds to sp^3 hybridization. The small amount of sp^3 hybridization is likely to be found primarily at the boundary regions of the petals, where many tiny twists and protuberances exist.[18] The third peak near 291 eV is broad and corresponds to carboxylate (O–C═C)[19] and confirms that adsorbed oxygen species are present on the surface of graphitic petals. The presence of oxygen is further confirmed by the Gaussian fit of the O 1s peak (inset in Fig. 2(b)). Quantitative analysis of the peak intensities indicates an atomic fraction of ~4% oxygen atoms on the graphitic petals. We also note that these Raman and XPS findings confirm the absence of any magnetic impurities in the graphitic petals.

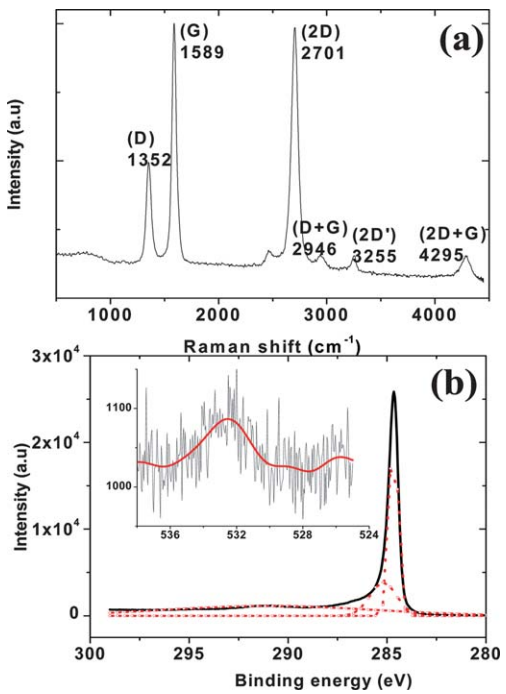

Fig. 2 (a) Raman spectrum of graphitic petals and (b) XPS spectra of C 1s and O 1s (inset) collected from the graphitic petals.

Fig. 3 shows the magnetization hysteresis loops of the petals measured at temperatures of 300 K, 100 K and 5 K respectively in the field range of -2.5 kOe < H < 2.5 kOe. Magnetization per unit volume has been calculated by considering the thickness of petal layer to be 500 nm. Ferromagnetic hysteresis from the petals is clearly apparent, with saturation of magnetization occurring at 4.7 emu cm^{-3} and a coercivity of 105 Oe at 300 K, which is much higher than the obtained magnetization in the case of few-layer graphene.[12,13] Small changes in saturation magnetization and coercivity at lower temperatures were observed, and at 5 K the saturation magnetization is 5.2 emu cm^{-3}. Estimated saturation magnetization per unit mass is 0.024, 0.0246 and 0.026 emu g^{-1} at 300, 100 and 5 K respectively. The inset of Fig. 3 contains the bare Si *M*–*H* curve subjected to the same thermal cycle, which clearly indicates diamagnetic behavior. These results demonstrate that the graphitic petals exhibit a weak ferromagnetic ordering at room temperature.

To better understand the origin of ferromagnetism in the petals and the effects of adsorbed oxygen species and vacancies, we have also measured the magnetic properties of petals grown with the addition of dilute oxygen (0.5 sccm oxygen flow during growth) under otherwise identical growth conditions to those described above. Fig. 4 shows the magnetic hysteresis curves obtained for the O_2 treated petals. These samples exhibit lower magnetization compared to samples grown without O_2, with saturation magnetizations of 2.1, 2.6 and 3.3 emu cm^{-3} at 300, 100 and 5 K respectively. Estimated saturation magnetization per unit mass is 0.017, 0.013 and 0.011 emu g^{-1} at 300, 100 and 5 K respectively. The coercivity is approximately 75 Oe at 300 K and 100 K, but at 5 K an enhanced coercivity of 450 Oe is observed for the O_2 treated petals. The reduction in magnetization might be to the result of lower vacancy density on the surface of the petals, though the observed change in magnetization in the case of the O_2 treated sample is not particularly large. Raman spectrum of the O_2 treated petals shows similar bands with I_D/I_G and I_G/I_{2D} ratios ~0.5 and 0.69 respectively (Fig. 5(a)). There is no significant change in the D-band intensity, but decrease in the 2D/G ratio suggests more number of graphene layers in the

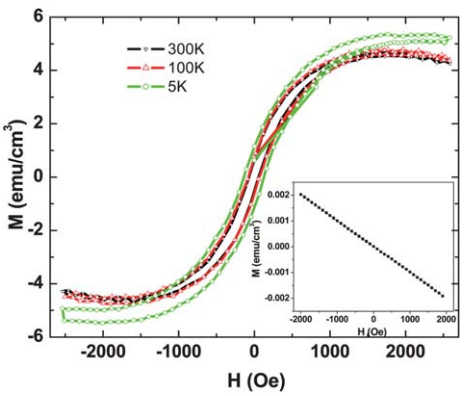

Fig. 3 Magnetization hysteresis loops obtained for graphitic petals (without O_2 treatment) at 300 K, 100 K and 5 K respectively. Inset shows magnetization *versus* field curve for the bare Si (100) substrate.

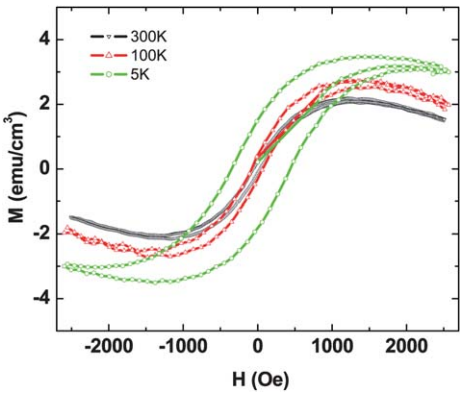

Fig. 4 Magnetization hysteresis loops obtained for graphitic petals (with O_2 treatment) at 300 K, 100 K and 5 K respectively.

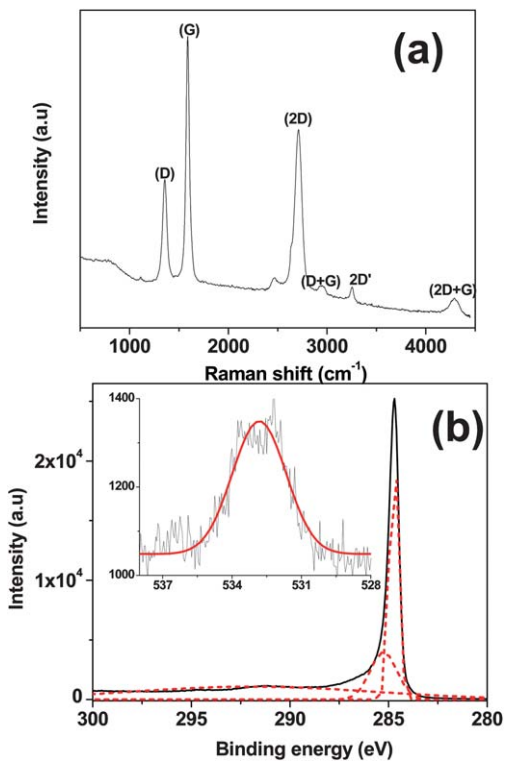

Fig. 5 (a) Raman spectrum and (b) XPS spectra of C 1s and O 1s (inset) collected from the O_2 treated graphitic petals.

petals. Hence, we believe that distribution of vacancy density is lowered in O_2 treated graphitic petals. XPS spectrum of the O_2 treated petals showed similar peaks with no significant changes, as observed for the petals grown without oxygen (Fig. 5(b)). The quantitative analysis of the Gaussian fitted O 1s peak shows atomic fraction of ~5.5% grafted oxygen species on O_2 treated graphitic petals. Fig. 6 shows the temperature-dependent magnetization of graphitic petal arrays at 1000 Oe grown with and without dilute O_2 and indicates that magnetization is enhanced for the O_2 treated sample at temperatures below 25 K.

Though the origin of ferromagnetism in carbon nanomaterials is not yet clear, various theoretical predictions and some experimental evidence have been offered recently to understand the

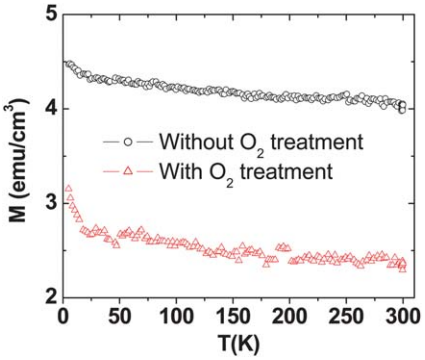

Fig. 6 Magnetization as a function of temperature of graphitic petals under application of a magnetic field of 1 kOe.

underlying mechanism(s).[20–22] Among them, proton irradiation experiments suggest that intrinsic carbon defects such as the lattice defects, vacancies, edges or topological defects and voids in the few-layer graphene give rise to localized magnetic states at the Fermi level, and the number of these states roughly scales with the defect perimeter.[23] Defects in few-layer graphene break the translational symmetry of the lattice and create localized states at the Fermi energy to produce an effective self-doping, where charge is transferred to/from defects to the bulk. In the presence of local electron–electron interactions, these localized states become spin-polarized, leading to the formation of local moments.[4]

DFT studies suggest that defects in graphite such as vacancies and hydrogen-terminated vacancies are magnetic, with a local magnetic moment larger than 1 μ_B occurring from long-range coupling of spin units that exist as defects.[5,9] Magnetic ordering and diamagnetic behavior are expected to be negligible in rolled graphene sheets, fullerenes and carbon nanotubes because they possess closed π-electron systems with no open edges.[24] Since our graphitic petal arrays have been grown without using any catalyst and no impurities are present in the sample, we believe that the magnetism arises predominantly from defects and vacancies formed during synthesis. Raman studies confirm that graphitic petals are highly defective. In particular, edge defects are expected to contribute significantly to the magnetic properties due to the high density of such edges ($\sim 4 \times 10^8$ interconnected petal edges in a 1×1 cm^2). Further detailed and theoretical studies are needed to fully understand these mechanisms.

In conclusion, we report room-temperature ferromagnetism of graphitic petal arrays grown without catalyst on Si substrates by MPCVD. The possible origin of ferromagnetism may originate from long-range coupling of spin due to edge defects and vacancies. Offering such a room-temperature ferromagnetic behavior, we believe that the petals could be used as elements in applications including magnetic memory, magnetoresistance and spintronic devices.

References

1 P. M. Allemand, K. C. Khemani, A. Koch, F. Wudl, K. Holczer, S. Donovan, G. Gruner and J. D. Thompson, *Science*, 1991, **253**, 301–302.
2 T. L. Makarova, B. Sundqvist, R. Honhne, R. Esquinazi, Y. Kopelvich, P. Scharff, V. A. Davydov, L. S. Kashevarova and A. V. Rakhmanina, *Nature*, 2001, **413**, 716–718.
3 T. L. Makarova, *Semiconductors*, 2004, **38**, 615–638.
4 P. O. Lehtinen, A. S. Foster, Y. Ma, A. V. Krasheninnikov and R. M. Nieminen, *Phys. Rev. Lett.*, 2004, **93**, 187202.

5 O. V. Yazyev and L. Helm, *Phys. Rev. B: Condens. Matter Mater. Phys.*, 2007, **75**, 125408.
6 R. F. Service, *Science*, 2004, **304**, 42–43.
7 H. Pardo, R. Faccio, F. M. Araujo-Moreira, O. F. de Lima and A. W. Mombru, *Carbon*, 2006, **44**, 565–569.
8 A. W. Mombru, H. Pardo, R. Faccio, O. F. de Lima, E. R. Leite, G. Zanelatto, A. J. C. Lanfredi, C. A. Cardoso and F. M. Araujo-Moreira, *Phys. Rev. B: Condens. Matter Mater. Phys.*, 2005, **71**, 100404 (R).
9 P. Esquinazi, D. Spemann, R. Hohne, A. Setzer, K.-H. Han and T. Butz, *Phys. Rev. Lett.*, 2003, **91**, 227201.
10 S. Talapatra, P. G. Ganesan, T. Kim, R. Vajtai, M. Huang, M. Shima, G. Ramanath, D. Srivastava, S. C. Deevi and P. M. Ajayan, *Phys. Rev. Lett.*, 2001, **95**, 097201.
11 J. Cervenka, M. I. Katsnelson and C. F. J. Flipse, *Nat. Phys.*, 2009, **5**, 840–844.
12 Y. Wang, Y. Huang, Y. Song, X. Zhang, Y. Ma, J. Liang and Y. Chen, *Nano Lett.*, 2009, **9**, 220–224.
13 H. S. S. R. Matte, K. S. Subrahmanyam and C. N. R. Rao, *J. Phys. Chem. C*, 2009, **113**, 9982–9985.
14 T. Bhuvana, A. Kumar, A. Sood, R. H. Gerzeski, J. Hu, V. S. Bhadram, C. Narayan and T. S. Fisher, *ACS Appl. Mater. Interfaces*, 2010, **2**, 644–648.
15 C. S. Rout, A. Kumar, G. Xiong, J. Irudayaraj and T. S. Fisher, *Appl. Phys. Lett.*, 2010, **97**, 133108.
16 C. N. R. Rao, A. K. Sood, K. S. Subrahmanyam and A. Govindaraj, *Angew. Chem., Int. Ed.*, 2009, **48**, 7752–7778.
17 S. J. Chae, F. Gunes, K. K. Kim, E. S. Kim, G. H. Han, S. M. Kim, H.-J. Shin, S.-M. Yoon, J.-Y. Choi, M. H. Park, C. W. Yang, D. Pribat and Y. H. Lee, *Adv. Mater.*, 2009, **21**, 2328–2333.
18 N. Jiang, H. X. Wang, H. Zhang, H. Sasaokac and K. Nishimura, *J. Mater. Chem.*, 2010, **20**, 5070–5073.
19 H. Ago, T. Kugler, F. Cacialli, W. R. Salaneck, M. S. P. Shaffer, A. H. Windle and R. H. Friend, *J. Phys. Chem. B*, 1999, **38**, 8117.
20 M. Otani, Y. Takagi, M. Koshino and S. Okada, *Appl. Phys. Lett.*, 2010, **96**, 242504.
21 W. Sheng, Z. Y. Ning, Z. Q. Yang and H. Guo, *Nanotechnology*, 2010, **21**, 385201.
22 T. Ma, F. Hu, Z. Huang and H.-Q. Lin, *Appl. Phys. Lett.*, 2010, **97**, 112504.
23 H. Ohldag, T. Tyliszczak, R. Hohne, D. Spemann, P. Esquinazi, M. Ungureanu and T. Butz, *Phys. Rev. Lett.*, 2007, **98**, 187204.
24 J. Heremans, C. H. Olk and D. T. Morelli, *Phys. Rev. B: Condens. Matter Mater. Phys.*, 1994, **49**, 15122–15125.